HHS Public Access

Author manuscript

Hum Brain Mapp. Author manuscript; available in PMC 2017 February 06.

Published in final edited form as:

Hum Brain Mapp. 2014 June ; 35(6): 2741–2753. doi:10.1002/hbm.22363.

The Role of Anterior Midcingulate Cortex in Cognitive Motor Control: Evidence From Functional Connectivity Analyses

Felix Hoffstaedter[1,2,*], **Christian Grefkes**[3,4], **Svenja Caspers**[1], **Christian Roski**[1], **Nicola Palomero-Gallagher**[1], **Angie R. Laird**[5], **Peter T. Fox**[6,7], and **Simon B. Eickhoff**[1,2]

[1]Institute for Neuroscience and Medicine (INM-1), Research Centre Jülich, Germany

[2]Institute of Clinical Neuroscience and Medical Psychology, Heinrich-Heine University, Düsseldorf, Germany

[3]Neuromodulation and Neurorehabilitation, Max-Planck-Institute for Neurological Research, Cologne, Germany

[4]Department of Neurology, University Hospital Cologne, Germany

[5]Department of Physics, Florida International University, Miami, Florida

[6]Research Imaging Institute, University of Texas Health Science Center, San Antonio, Texas

[7]Research Service, South Texas Veterans Administration Medical Center, San Antonio, Texas

Abstract

The rostral cingulate cortex has been associated with a multitude of cognitive control functions. Recent neuroimaging data suggest that the anterior midcingulate cortex (aMCC) has a key role for cognitive aspects of movement generation, i.e., intentional motor control. We here tested the functional connectivity of this area using two complementary approaches: (1) resting-state connectivity of the aMCC based on fMRI scans obtained in 100 subjects, and (2) functional connectivity in the context of explicit task conditions using meta-analytic connectivity modeling (MACM) over 656 imaging experiment. Both approaches revealed a convergent functional network architecture of the aMCC with prefrontal, premotor and parietal cortices as well as anterior insula, area 44/45, cerebellum and dorsal striatum. To specifically test the role of the aMCC's task-based functional connectivity in cognitive motor control, separate MACM analyses were conducted over "cognitive" and "action" related experimental paradigms. Both analyses confirmed the same task-based connectivity pattern of the aMCC. While the "cognition" domain showed higher convergence of activity in supramodal association areas in prefrontal cortex and anterior insula, "action" related experiments yielded higher convergence in somatosensory and premotor areas. Secondly, to probe the functional specificity of the aMCC's convergent functional connectivity, it was compared with a neural network of intentional movement initiation. This exemplary comparison confirmed the involvement of the state independent FC network of the aMCC in the intentional generation of movements. In summary, the different experiments of the

[*]Correspondence to: Felix Hoffstaedter, Institute of Neuroscience and Medicine (INM-1), Research Centre Jülich, D-52425 Jülich, Germany. f.hoffstaedter@fz-juelich.de.

Additional Supporting Information may be found in the online version of this article.

present study suggest that the aMCC constitute a key region in the network realizing intentional motor control.

Keywords

cognitive motor control; fMRI; meta-analytic connectivity modeling; anterior midcingulate cortex; seed based resting-state analysis

INTRODUCTION

Brodmann's cytoarchitectonic map [1909] of the human brain divided the cingulate cortex into the precingulate (classical anterior cingulate cortex: ACC) and the postcingulate (posterior cingulate cortex: PCC) subregion. In 2004, Vogt et al. then introduced an influential four region model of the cingulate cortex (Fig. 1) based on structural and functional evidence in humans and primates. This model subdivided the classical ACC into the rostral ACC and the midcingulate cortex (MCC). Interestingly, the anterior part of the latter region (aMCC) is one of the most frequently activated brain structures in functional neuroimaging [Yarkoni et al., 2011]. It is involved in numerous different contexts from self-initiated finger tapping [Deiber et al., 1999] to reward-based decision making [Bush et al., 2002] as well as processing of pain and negative affect [Shackman et al., 2011]. This functional diversity is reflected by the variety of theoretical considerations on the mental processes that may be sustained by this area. Among these, one influential set of theories claim that the aMCC crucially contributes to cognitive control by conflict detection [Carter et al., 1998] and conflict monitoring [Botvinick et al., 2004]. An alternative account of aMCC functioning would be that it is essential for the preparation and implementation of potential actions (readiness for action) realizing adaptive control [Shackman et al., 2011] and conflict resolution to this end. In line with this view, a recent fMRI study demonstrated overlapping neural activity in a part of the aMCC for simple movement selection and free timing of movement initiation [Hoffstaedter et al., 2013], suggesting that the aMCC plays an essential role in intentional motor control. Ample evidence functionally links the aMCC with prefrontal, premotor and parietal areas as well as the basal ganglia forming a core network for the internal generation of movements [Cunnington et al., 2002; Debaere et al., 2003; Deiber et al., 1999; Jankowski et al., 2009; Lau et al., 2004; van Eimeren et al., 2006]. It may thus be hypothesized that the aMCC is crucial for the implementation of intentional motor control by translating abstract cognition and intentions to actions and connecting cognitive and motor systems [Paus, 2001]. Accordingly, the aMCC should be connected with both cognitive and motor-related neural networks. In the current study, we addressed this question by investigating the functional connectivity (FC) of a functionally defined part of the aMCC associated with intentional movement generation [Hoffstaedter et al., 2013] applying two complementary approaches [cf. Eickhoff and Grefkes, 2011]. First, FC was assessed in the context of explicit task conditions by performing meta-analytic connectivity modeling (MACM), which delineates significant co-activations across a broad range of experimental paradigms. Secondly, a "resting-state" connectivity analysis was conducted to delineate FC of the aMCC region during absence of an external task, that is, in an endogenously controlled state of unconstrained mind-wandering. Separate MACM analyses

over “cognitive” and “action” tasks were additionally performed to further address the hypothesis that the aMCC is involved in both cognitive related and motor related neural systems. A conjunction across task-dependent and task-independent FC analyses was then performed to yield FC patterns of the aMCC region independent of current “state.” Finally, to probe the functional specificity of this state independent FC network, it was compared with a neural network associated with intentional movement initiation, which represents a prototypical interaction between cognitive and motor functions [Haggard, 2008].

MATERIALS AND METHODS

Seed Region

The seed region for the following analyses was taken from a recent fMRI study which examined neural effects of self-initiated movements by letting subjects choose between left or right finger movements to be initiated at an freely chosen point in time [Hoffstaedter et al., 2013]. A part of the aMCC (areas a24′, 32′ [Palomero-Gallagher et al., 2009]; Fig. 2) was found to be the only brain region showing increased activity not only for movement selection but additionally for the free timing of movement initiation. This functionally defined volume of interest (VOI) associated with intentional movement initiation is used here as seed for the FC analyses (center of mass $x = -3$, $y = 18$, $z = 42$; volume = 1,873 mm^3). It should be noted, that the entire volume of this cluster was used to define the seed, rather than considering only its peak location. This approach is based on findings from a comprehensive simulation approach to FC [Smith et al., 2011] which recently showed that functional specific seed VOIs provide better results for modeling functional networks than atlas based VOIs or single points.

Meta-Analytic Connectivity Modeling

Meta-analytic connectivity modeling (MACM) is a relatively new approach to the analysis of functional connectivity [Friston et al., 1993] based on correlations of neural activity in different brain areas over studies, i.e., co-activation. For doing so, MACM draws upon the advantage of high standardization in the publication of neuroimaging data, e.g., the ubiquitous adherence to standard coordinate systems (Talairach, MNI) and the emergence of large-scale databases that store this information. The key idea behind MACM is to first identify all experiments in a database that activate a particular brain region (seed/VOI), and then test for convergence across (all) activation foci reported in these experiments [Laird et al., 2009]. Obviously, as experiments were selected by activation in the seed, highest convergence will be observed in the seed region. Significant convergence of the reported foci in other brain regions, however, indicates consistent co-activation over experiments with the seed region. In contrast to the more prevailing time-series approach to FC [Van Dijk et al., 2010], the unit of observation in MACM is thus not a specific point in an acquired time-series but a particular neuroimaging experiment. MACM therefore extends the scale on which FC is evaluated beyond individual studies to delineate neural networks that are conjointly recruited over various independent experiments. Moreover, it should be noted that MACM as a data-driven approach characterizes the co-activations of a given region of interest—independent of how this seed has been defined. That is, while MACM has most commonly been used to investigate the functional connectivity of anatomically defined seed

regions [Cauda et al., 2011; Eickhoff et al., 2010; Robinson et al., 2010], brain regions defined by functional properties as in the current study, may likewise be assessed [Jakobs et al., 2012].

To identify studies reporting neural activation within the aMCC region, the BrainMap database was employed (www.brainmap.org [Fox and Lancaster, 2002; Laird et al., 2005]), which did not contain any results of the study the seed VOI was taken from. To date, this database contained activation coordinates from over 10,000 neuroimaging experiments. Only imaging studies, which examined task-based activations in a group of healthy subjects, were considered, while between-group contrasts, patient populations and intervention-studies were excluded. These criteria yielded ~6,500 eligible experiments at the time of analysis. As the first step of the MACM analysis we identified all experiments that featured at least one focus of activation within the aMCC VOI (in MNI-space). In order to facilitate such filtering, coordinates from all experiments in the BrainMap database reporting their results in Talairach space were converted into MNI coordinates by using the Lancaster transformation [Lancaster et al., 2007]. Then, all experiments activating the currently considered seed were identified. The retrieval was solely based on the reported activation coordinates, not on any anatomical or functional label. The convergence of reported neural activation across those experiments featuring at least one focus of activation within the seed volume was then modeled using the revised version of the activation likelihood estimation (ALE) algorithm [Eickhoff et al., 2009].

The ALE approach is based on modeling the coordinates reported in the identified experiments as centers of 3D Gaussian probability distributions. These modeled activation fields reflect spatial uncertainties due to between-subject variability but also to partially differing parameters in imaging methods and data analysis of the single imaging experiments (between-template variance). For each experiment, the probability distributions of all reported foci are combined into a modeled activation (MA) map [Turkeltaub et al., 2012]. Taking the union across these MA maps yields voxel-wise ALE scores. The resulting ALE map represents a quantitative description of activity convergence over all experiments at each particular location of the brain. To distinguish “true” convergence from random convergence, ALE scores are compared with an empirical null distribution reflecting a random spatial association between experiments (random effects analysis [Eickhoff et al., 2012]). The ALE maps reflecting the convergence of co-activations with the aMCC were family wise error (FWE) corrected at a cluster level threshold of $P<0.05$ (cluster-forming threshold: $P<0.001$ at voxel level; cluster extend threshold $k=211$), and converted to Z-scores for visualization.

Importantly, in the BrainMap database each experiment is associated with a specific “Behavioral Domain” which classifies the mental operations isolated by the experimental contrast [Laird et al., 2005]. The specific behavioral domain is coded by the intent of the experimental design and divided into six main categories: cognition, emotion, perception, interoception, action, and pharmacology. Based on this coding scheme we were able to directly test whether the aMCC is integrated with both cognitive and motor-related neural networks by separately analyzing co-activations of the VOI for those among the identified experiments that were categorized as either “cognition” or “action,” respectively [cf. Laird et

al., 2009]. In these follow-up analyses, we repeated the above procedure but this time only considered those experiments in the Brain-Map meta-data that were assigned to either cognitive or motor (action) related processes. To test for commonalities of both analyses under these conditions, we calculated the conjunction over the two ALE maps. Differences between both MACMs were assessed by first calculating the voxel-wise differences of the *Z*-scores obtained from the inspected ALE-maps. The experiments contributing to either analysis were then pooled and randomly divided into two groups of the same size as the sets of contrasted experiments [Eickhoff et al., 2011]. Voxel wise ALE scores for these two randomly assembled groups were subtracted from each other and recorded. Repeating this process 1,000 times yielded an empirical null distribution of ALE-score differences between the two conditions ("cognition" vs. "action") [Rottschy et al., 2012]. The map of "true" differences between two MACMs was tested against this null-distribution yielding a posterior probability that the true difference was not due to random noise in an exchangeable set of labels, based on the proportion of lower differences in the random exchange. The resulting probability values were thresholded at $P > 0.95$ (95% chance for true difference) and an additional cluster extend threshold of $k = 211$ voxels was applied, taken from the original MACM over all experiments with aMCC activation. The resulting contrasts between MACMs yielded areas of higher relative consistency of co-activation with the aMCC VOI represented by clusters of significantly higher activation likelihood of the respective behavioral domain: "cognition" or "action."

Seed Based Resting-State Analysis

In addition to the MACM analysis, task-independent FC of the aMCC region was investigated by means of a seed based resting-state analysis. Complementary to the MACM approach, this analysis of FC focuses on correlated fluctuations in the time-series of neural activity as represented by the BOLD-signal within distinct parts of the human brain at "rest" [Biswal et al., 1995]. Resting-state fMRI images were acquired in 100 healthy volunteers (50 females; age range 22–71 years, mean 45.3 ± 14.1), all of which were right handed according to the Edinburgh handedness inventory [Oldfield, 1971]. All subjects gave written informed consent to the study protocol, which had been approved by the local ethics committee. Before the imaging session, subjects were instructed to keep their eyes closed and just let their mind wander without thinking of anything in particular and not to fall asleep, which was confirmed by post-scan debriefing. Blood oxygen level dependent (BOLD) signals were acquired using echo-planar imaging (EPI) on a Siemens Tim Trio 3T whole-body scanner (Erlangen, Germany) at the Research Centre Jülich in Germany. For each subject, 300 whole brain volumes were acquired (gradient-echo EPI pulse sequence, TR = 2.2 s, TE = 30 ms, flip angle = 90°, in plane resolution = 3.1 x 3.1 mm, 36 axial slices of 3.1 mm thickness). The first four images were discarded to allow for magnetic field saturation, before the remaining 296 were preprocessed using SPM8 (www.fil.ion.ucl.ac.uk/spm). First, images were corrected for head motion by affine registration using a two-pass procedure registering all images to the individual mean of the respective subject. The mean image was then spatially normalized to the MNI single subject template [Holmes et al., 1998] using the "unified segmentation" approach [Ashburner and Friston, 2005]. The ensuing deformation was then applied to the individual EPI volumes. Finally, images were

smoothed by a 5-mm FWHM Gaussian kernel to meet requirements of normal distribution and compensate for residual anatomical variations.

In order to reduce spurious correlations, variance that could be explained by the following nuisance variables was removed from each voxel's time series [cf. Jakobs et al., 2012; Weissenbacher et al., 2009; zu Eulenburg et al., 2012] applying a GLM approach: (i) the six motion parameters derived from the image realignment; (ii) the first derivative of the realignment parameters; (iii) mean grey and white matter as well as CSF signal intensity; (iv) coherent signal changes across the whole brain as reflected by the first five components of a PCA decomposition of the whole-brain time-series (CompCor denoising [Behzadi et al., 2007; Chai et al., 2012]). All nuisance variables entered the model as first, and all but the PCA components also as second order terms, which were shown to increase specificity and sensitivity of the analyses. Finally, the data was band pass filtered between 0.01 and 0.08 Hz [Cordes et al., 2001].

Identically to the MACM analysis, the functionally defined aMCC region was used as seed VOI in the resting-state analysis. In particular, the time-course of the seed for every subject was extracted from the seed volume by computing the first eigenvariate of the time-series of those 50% of the seed's gray matter voxels (median split) that had the highest probabilities of representing grey matter according to the SPM8 segmentation. To quantify resting-state FC, linear (Pearson) correlation coefficients were computed between the representative time series of the VOI and those of all other grey matter voxels in the brain. The voxel-wise correlation coefficients were then transformed into Fisher's Z-scores and tested for consistency across subjects by a second-level analysis of variance (ANOVA, including appropriate nonsphericity correction). The results of this random-effects analysis were family wise error (FWE) corrected at a threshold of $P<0.05$.

Consistent Functional Connectivity of the Midcingulate Cortex

In order to delineate brain regions showing FC with the aMCC region in task-dependent (MACM) as well as in task-free states (resting-state), a conjunction analysis over both connectivity analyses was performed using the conservative minimum statistic [Nichols et al., 2005]. That is, consistent FC independent of context was analyzed by computing the intersection of the thresholded (including correction for multiple comparisons) functional connectivity maps obtained by MACM and the seed based resting-state analysis [Jakobs et al., 2012]. In a second step, to probe the functional specificity of this state independent FC network, it was related to neural correlates of intentional generation of behavior [Haggard, 2008], which may be considered prototypically for the interaction between cognitive and motor functions. Therefore, the overall FC pattern was compared with neural correlates of self-initiated movements examined in a recent fMRI study with 35 healthy subjects [Hoffstaedter et al., 2013]. It should be noted that, even though the neural correlates of intentional movement generation were derived from the same study as the seed for the FC analyses, the contrast yielding the aMCC activation tested for an increase of neural activity over three conditions (1. Free >2. Choice >3. Reaction). This specific contrast was exclusively significant for the aMCC seed VOI, which in context of the fMRI experiment was thus discussed as a key node for the intentional initiation of behavior. Relevant for the

current study was the question, whether the neural correlates of intentional movement generation (compared with reactive movements) match the state-independent FC network of the aMCC. This was tested by computing the conjunction over the contrast between self-initiated (free hand choice and timing) and reactive movements from the previous fMRI study (cluster-level FWE corrected at $P<0.05$; [Hoffstaedter et al., 2013]) and the overall FC map of the aMCC seed. This conjunction delineated regions of significant task-based (MACM) and task-independent (resting-state) functional connectivity with the aMCC that are at the same time also significantly stronger activated by self-initiated versus reactive movements. To ensure that the conjunction yields results corrected for multiple comparisons, we additionally used the conservative approach of implementing an additional cluster threshold of 211 voxels, which corresponds to the cluster-FWE correction of the global MACM analysis over 656 experiments. As a matter of completeness and to test for functional specificity of the aMCC VOI, we calculated additional MACMs for all regions included in the resulting "core network" (Supporting Information Figure S1) and computed conjunctions over these MACMs (Supporting Information Figure S2). The results are depicted in the supplementary material. Anatomical assignment of resulting brain areas was performed via the SPM Anatomy toolbox (www.fz-juelich.de/ime/spm_anatomy_toolbox, V1.8 [Eickhoff et al., 2007]), which is based on various cytoarchitectonic studies providing maximum probability maps of several brain areas [cf. Zilles and Amunts, 2010]. Details on these regions base on cyto- and receptor architectonics may be found in the following publications reporting on Broca's region [Amunts et al., 1999], inferior frontal junction [Amunts et al., 2010], anterior and midcingulate cortex [Palomero-Gallagher et al., 2008, 2009], premotor cortex [Geyer et al., 1996], primary motor [Geyer et al., 1996] and sensory cortex [Geyer et al., 2000], fusiform gyrus [Caspers et al., 2013], inferior parietal cortex [Caspers et al., 2008], superior parietal cortex and intraparietal sulcus [Caspers et al., 2008; Choi et al., 2006; Scheperjans et al., 2008]. Regions, which are not yet cytoarchitectonically mapped based on observer-independent histological examination, were labeled macroanatomically by the probabilistic Harvard-Oxford cortical structure atlas.

RESULTS

Task Based Functional Connectivity

The VOI search in the BrainMap database revealed 656 experiments containing activation foci within the aMCC seed, which directly reflects the raw data of the location-based search in the BrainMap database, without additional manipulations. Importantly, the study form which the seed VOI originated was not included in the BrainMap database. The subsequent ALE over all coordinates reported by these studies revealed convergent co-activation in a large-scale network consisting of MCC (aMCC: areas a24′, 32′; pMCC: area p24′), supplementary motor area (SMA: area 6), pre-SMA, DLPFC, lateral premotor cortex, intraparietal sulcus (IPS: areas hIP1–3), superior (SPL: areas 7A, left 7PC) and inferior parietal lobule (IPL: areas PFt, PFm; left areas PFop, PF, PFcm) together with area 44 and 45, inferior frontal junction (IFJ: areas IFJ1,2), anterior insula (aIns), fusiform gyrus (FG: areas FG1,2), left primary motor area (M1: area 4a), left primary sensory area (S1: area 3b) and left middle temporal gyrus (Fig. 3A). Subcortical areas featuring functional connectivity

with the aMCC were bilateral putamen, caudate nucleus, pallidum, thalamus, and cerebellum.

Of all experiments featuring activation in the aMCC, 42% were attributed to the behavioral domain “cognition” (277 experiments; Fig. 3B) and 34% to the “action” domain (222 experiments; Fig. 3C). The remaining ~24% were associated with other behavioral domains such as perception or emotion. The conjunction over both MACMs including experiments with the behavioral domain “cognition” and “action” (Fig. 3D), respectively, featured convergent co-activation in the same but reduced network as the original MACM over all 656 experiments including the aMCC to SMA cluster, but leaving out area 45, IPL and most of the DLPFC. When contrasting both MACMs, experiments with the behavioral domain “cognition” (Fig. 3E) featured significantly more consistent co-activation in bilateral DLPFC, IFJ (IFJ1 and left IFJ2), aIns, rostral aMCC (areas a24′, 32′), left dorsomedial area 44 and area 45, left IPS (area hIP3) and left FG (area FG2). Experiments from the behavioral domain “action” in turn (Figure 3F) featured significantly more consistent co-activation with primary motor (M1: areas 4a, left area 4p) and primary sensory (S1: area 3b) cortices, parietal operculum (OP4), lateral premotor cortex, SMA (area 6), pre-SMA, MCC (areas a24′, p24′), area 44, IPL (area PFt; right areas PF, PFcm) and left SPL (areas 7A, 7PC) as well as thalamus, putamen and the cerebellum.

Task Free Functional Connectivity

The resting-state analysis revealed a large-scale network of correlated activity with the aMCC seed VOI (Fig. 4) comprising MCC (aMCC: area a24′, 32′; pMCC: area p24′), SMA (area 6), pre-SMA, left area 45 and bilaterally in DLPFC, dorsolateral premotor cortex, aIns, area 44, IFJ (areas IFJ1,2), IPS (areas hIP1–3), IPL (areas PF, PFm; left area PFt), and left SPL (area 7A). Subcortically, the aMCC seed showed correlations with the caudate nucleus, anterior putamen, pallidum, nucleus accumbens, bed nucleus, thalamus, and cerebellum in both hemispheres.

Overall Functional Connectivity

Consistent FC of the aMCC independent of the current state (task-driven vs. task-free) was identified by combining the two complementary connectivity analyses described above. To this end we assessed the conjunction over the aMCC’s FC in context of explicit task conditions, represented by the MACM over all experiments activating the aMCC seed region, and the aMCC’s FC in the absence of an external task represented by the seed-based resting state analysis. The resulting overall FC network of the aMCC seed comprises MCC (aMCC: areas a24′, 32′, pMCC: area p24′), SMA (area 6), pre-SMA and left area 45 together with DLPFC, area 44, IFJ (areas IFJ1,2), aIns, lateral premotor cortex, IPL (area PFm; left area PFt) and IPS (area hIP1–3)—all in both hemispheres (Fig. 5A). Caudate nucleus, pallidum, anterior putamen, thalamus and cerebellum were also identified bilaterally as consistently connected to the aMCC region.

To probe the functional specificity of this FC pattern independent of context, the result of the above analysis was compared with neural correlates of intentional movement generation as identified in an fMRI study in 35 healthy subjects [Hoffstaedter et al., 2013]. In this study,

contrasting neural activity related to self-initiated movements with activity related to (closely matched) reactive movements yielded the neural correlate of intentional action as the contrast eliminates purely movement related neural activity [Haggard, 2008]. The areas involved were aMCC (areas a24′, 32′), SMA (area 6), pre-SMA, right IFJ (areas IFJ1,2) and right area 45 as well as bilateral DLPFC, area 44, aIns, dorsolateral premotor cortex, IPL (areas PFm, PFt; left area PF; right area PGa), IPS (areas hIP1–3), SPL (area 7PC; right areas 7P, 7A), caudate nucleus, pallidum, putamen and cerebellum (Fig. 5B). Notably, intentional movement initiation yielded increased neural activity in virtually the same brain regions involved in the aMCC seed's overall FC network. This observation was quantitatively verified by the conjunction over both networks which identified convergent connectivity with the aMCC region in the task-driven and task-free state as well as functional recruitment by volitional motor control in a "core network" that comprised the aMCC (areas a24′, 32′), SMA (area 6), pre-SMA, DLPFC, dorsolateral premotor cortex, area 44, aIns, IPL (area PFm; left area PFt), IPS (area hIP1–3), cerebellum, anterior putamen and the right caudate nucleus (Fig. 5C). For illustrative purposes, the separate conjunctions over MACM and self-initiated movements as well as over resting-state connectivity and the latter are included as Supporting Information (Fig. S3).

DISCUSSION

In the current study, we examined the task-dependent and task-independent functional connectivity of a functionally defined aMCC region, which represents a key area for intentional motor control. Convergent results of meta-analytic connectivity modeling (MACM) and resting-state correlation analyses seeded from the aMCC region showed that a specific pattern of FC was equally present in states where subjects had to engage in structured, externally specified tasks as well as in a task-free, endogenously controlled "resting" state. In particular, in both states, the aMCC seed was significantly coupled with a large-scale network comprising DLPFC, IPS, IPL, aIns, area 44/45, dorsolateral premotor cortices, SMA and pre-SMA as well as cerebellum, anterior putamen and the caudate. The current results are well in line with previous investigations of resting-state FC, which used anatomically defined seeds throughout the ACC/MCC [Kelly et al., 2009; Margulies et al., 2007; Yu et al., 2011], rather than a functionally derived and, hence, functionally specific seed region used here. Additionally, Beckmann et al. [2009] used diffusion weighted MRI to estimate anatomical connectivity between cingulate cortex and several target regions, also revealing interconnection of the aMCC with DLPFC, premotor cortex, and the dorsal striatum.

Separate MACM analyses constrained to experiments probing mental operations of either "cognition" or "action" (as coded in the BrainMap database) revealed a very similar, slightly reduced task-based FC network like the original MACM over all experiments. The comparison between these MACMs revealed higher convergence of co-activation for "cognition" in contrast to "action" mainly in higher-order and multimodal association areas like DLPFC, IFJ and aIns. For experiments examining "action" on the other hand the aMCC region was significantly connected to primary somatosensory and premotor cortices as well as bigger parts of motor related subcortical areas. Finally, the overall FC network of the aMCC VOI also showed increased neural activity for self-initiated movements relative to

reactions [Hoffstaedter et al., 2013]. Taken together, this task-related and specific functional evidence supports the view of the aMCC as part of a state independent neural "core network" realizing intentional motor control and action.

Conceptional Considerations on Functional Connectivity

Functional connectivity (FC) reflects the temporal correlation of spatially distinct neurophysiological events [Friston et al., 1993]. Here, we applied two different methods to examine complementary aspects of FC related to different mental states or modes: MACM assesses task-dependent FC, whereas seed based resting-state analysis accounts for task-free FC. The first approach made use of the BrainMap database [Laird et al., 2009] to determine convergent task based (stimulus-evoked) neural co-activation with the aMCC VOI across a large variety neuroimaging experiments [cf. Eickhoff et al., 2010]. Secondly, we assessed correlated fluctuations of the BOLD-signal within the aMCC region and other brain areas in order to identify regions of significant functional coupling with this seed region in a task free (resting-) state [cf. Van Dijk et al., 2010]. It has long been conjectured that regions functionally connected in a resting-state also co-activate in functional neuroimaging studies and vice versa [Biswal et al., 1995; Fox and Raichle, 2007]. This correspondence was corroborated by Smith et al. [2009] showing good concordance of independent component analyses (ICA) on BrainMap and resting-state data, respectively. The authors concluded that functional networks active in specific task conditions are continuously and dynamically utilized by the brain at "rest". The reference to different measures of FC additionally enables inference of FC independent of the current "mental state" (task related; endogenously controlled). Moreover, given that a combination of different methods should be less susceptible to drawbacks inherent in each individual method (MACM, resting-state analysis), the conjunction analyses should moreover represent a conservative approach to FC [Eickhoff et al., 2011; Jakobs et al., 2012; Reetz et al., 2012; Smith et al., 2009]. The current study showed close correspondence between FC networks in both states for the functionally defined aMCC VOI, which points to fundamental functional characteristics of the neural network revealed by FC analyses rather than effects stemming from a particular mental state (task vs. rest).

Organization of the Midcingulate Cortex

Brodmann's pre-cingulate subregion (classical ACC [Brodmann, 1909]) has later been subdivided into two qualitatively distinct brain regions [for review see Vogt, 2009b] based particularly on neuroanatomical information in nonhuman primates. For example, invasive tract tracing in rhesus monkeys demonstrated that the amygdala is anatomically connected only to the ACC and the aMCC [Vogt and Pandya, 1987] whereas the posterior MCC (pMCC) and the PCC are connected to the inferior parietal cortex. Combining tract tracing and cytoarchitecture in macaque monkeys, Dum and Strick [1991] found direct projections to the spinal cord originating from the pMCC. Cytoarchitectonic characteristics of the MCC were largely replicated for the human brain [Vogt et al., 2003; Vogt and Vogt, 2003] highlighting the similarity of this region with medial premotor regions (pre-SMA, SMA). Functionally, the analysis of nociceptive activations of the human brain revealed that the MCC is a major location for pain-processing and in particular its anterior part is associated with fear and anxiety, critical for avoidance behavior [Vogt et al., 2003]. Subsequently, Vogt

proposed the four-region neurobiological model of the cingulate cortex which comprises ACC, MCC (combined forming the classical ACC/Brodmann's precingulate subregion), PCC and retrosplenial cortex reflecting its circuitry and functional organization (Fig. 1 [Vogt, 2005; Vogt et al., 2004]). With respect to the current study, the constitutive distinction between ACC and MCC was validated by extensive cytoarchitectural [Palomero-Gallagher et al., 2008] and multireceptor mapping [Palomero-Gallagher et al., 2009] in humans.

For the human brain, in contrast to the experimental possibilities with animals, anatomical connectivity cannot be directly assessed, although probabilistic fiber tracking based on diffusion weighted MRI provides decent estimates of axonal connections between brain areas [Johansen-Berg and Rushworth, 2009]. This fact illustrates the importance of invasive tract tracing studies in monkeys to refer to "true" anatomical connections between areas in the monkey brain, which may then be used to infer connections of presumably homologous areas in the human brain. Caspers et al. [2011] for example showed close similarities between probabilistic fiber tracing seeding from different areas in the human IPL and axonal connectivity pattern of the IPL in macaque monkeys as revealed by tracer studies. Using retrograde tract tracing in macaques, Morecraft et al. [2012] found the aMCC to be structurally connected with SMA, pre-SMA, premotor and other cingulate areas as well as with various parts of the prefrontal cortex, insula and superior temporal cortex, dorsolateral parietal cortex, the medial parietal region and limbic regions. This pattern of anatomical connectivity of the aMCC in monkeys largely corresponds to results from probabilistic tractography in humans [Beckmann et al., 2009] and is also in line with the results of our FC analyses of an aMCC subregion in humans. Considering interspecies comparisons, it has to be noted that the human brain features obvious differences to the monkey brain, which is specifically the case for the aMCC, as monkeys do not have an area 32′ [Vogt, 2009a]. Reviewing structural and function data on the MCC from humans and monkeys, Cole et al. [2009] suggested that the additional area 32′ in humans might provide additional behavioral functions and increasing cognitive flexibility in humans relative to monkeys.

In general, good convergence was found between structural (probabilistic tracing) and functional (resting-state and MACM) connection pattern [Eickhoff et al., 2010; Greicius et al., 2009] and FC seems positively correlated with structural connectivity strength [Damoiseaux and Greicius, 2009]. However, it is commonly the case that strong functional connections also exist between brain regions with no direct structural connection [Honey et al., 2009]. Consequently, one should not equate structural and functional connectivity, as FC may be mediated by indirect structural connections, e.g. via a third region or more complex loops. Furthermore, the specific functionally defined aMCC VOI analyzed here as part of the midcingulate cortex, should be carefully distinguished from the extensive and heterogeneous region with the rather ill-defined "anterior cingulated" label. Finally, the specific FC pattern observed in the current study may be a specific functional feature of the human aMCC, which despite the mentioned restrictions largely resembles the structural connectivity found with diffusion imaging [Beckmann et al., 2009].

Function of the Midcingulate Cortex

A recent fMRI study found evidence for a critical role of a specific part of the aMCC (mean MNI coordinates: $x = -3$; $y = 18$; $z = 42$) in intentional movement initiation [Hoffstaedter et al., 2013]. In particular, this study examined intentional movement generation by combining the free choice of a hand to move with the internal timing of movement execution in contrast to closely matched reactions to exclude purely movement related neural activity. The exclusive overlap between internal timing and movement selection was found in the aMCC VOI, suggesting a key role of this area in intentional, i.e. cognitive, motor control. Virtually the identical region was also found by Shackman et al. [2011] in a quantitative meta-analyses to feature overlapping activity for the three domains: cognitive control, pain, and negative affect (Talairach coordinates: $x = 0$, $y = 12$, $z = 42$; MNI-transformation [Lancaster et al., 2007]: $x = 1$, $y = 17$, $z = 41$). In their review, the authors concluded that computational models of cognitive control and reinforcement learning may account for this region's contribution to negative affect and pain. In turn, the current study underlines that the aMCC is closely associated with cognitive motor control. The likewise reported involvement in the context of negative affect and pain hence needs to be addressed. On the level of basic cognition, both pain and negative affect normally induce the strong intention to control the effective context in order to change the physically or emotionally painful situation. Thus, pain and negative affect result in activation of the cognitive control system and the "readiness for action", which crucially includes the aMCC. Regarding structural connectivity, Paus [2001] emphasized the aMCC's strategic anatomical position beside its functional role in motor control, cognition and "arousal/drive states" of the organism as ideal prerequisites to translate intentions to actions. This consideration is supported on the functional level by the separately calculated MACMs over experiments with aMCC activation involving neural systems for "cognition" and "action," respectively. Both analyses revealed the premotor and midcingulate cortex, area 44, anterior insula, supplementary and presupplementary motor area, dorsal striatum, thalamus and the cerebellum all bilaterally to feature task-base FC with the aMCC. Together with the DLPFC, these areas in terms of a "core network" represent a neural correlate of intentional motor control [Haggard, 2008].

Furthermore, contrasting cognitive tasks to "action" tasks, the aMCC co-activated more consistently the highly integrative areas DLPFC [Koechlin and Summerfield, 2007], IFJ [Brass et al., 2005], and the aIns [Kurth et al., 2010]. On the other hand, only the task-based FC network for "action" included the primary somatosensory cortex and showed significantly stronger involvement of premotor areas, putamen, thalamus and the cerebellum. Nevertheless, the conjunction over both tasks included most of the "core network" with aMCC to SMA region, except for the DLPFC. Taken together, the domain specific MACM analyses may be interpreted in favor of the initial hypothesis stating that the aMCC represents a crucial node in the neural network recruited for the implementation of intentions as immediate behavior.

CONCLUSION

In summary, the current study demonstrates strong convergence between task dependent (MACM) and resting-state functional connectivity of the functionally defined aMCC region.

This convergent, state independent functional connectivity pattern closely corresponds to the network involved in intentional movement generation [Hoffstaedter et al., 2013] suggesting a key role of this functional "core network" in realizing intentional motor control. The comparative MACMs of the "cognition" and "action" domain as assigned in the BrainMap database support the notion of a crucial involvement of the aMCC in both cognitive and motor execution related functional systems. Thus, we provide evidence that the aMCC is functionally coupled to this entire (core) network implementing cognitive motor control.

Supplementary Material

Refer to Web version on PubMed Central for supplementary material.

References

Amunts K, Lenzen M, Friederici AD, Schleicher A, Morosan P, Palomero-Gallagher N, Zilles K. Broca's region: Novel organizational principles and multiple receptor mapping. PLoS Biol. 2010; 8:e1000489. [PubMed: 20877713]

Amunts K, Schleicher A, Burgel U, Mohlberg H, Uylings HB, Zilles K. Broca's region revisited: cytoarchitecture and intersubject variability. J Comp Neurol. 1999; 412:319–341. [PubMed: 10441759]

Ashburner J, Friston KJ. Unified segmentation. Neuroimage. 2005; 26:839–851. [PubMed: 15955494]

Beckmann M, Johansen-Berg H, Rushworth MF. Connectivity-based parcellation of human cingulate cortex and its relation to functional specialization. J Neurosci. 2009; 29:1175–1190. [PubMed: 19176826]

Behzadi Y, Restom K, Liau J, Liu TT. A component based noise correction method (CompCor) for BOLD and perfusion based fMRI. Neuroimage. 2007; 37:90–101. [PubMed: 17560126]

Biswal B, Yetkin FZ, Haughton VM, Hyde JS. Functional connectivity in the motor cortex of resting human brain using echo-planar MRI. Magn Reson Med. 1995; 34:537–541. [PubMed: 8524021]

Botvinick MM, Cohen JD, Carter CS. Conflict monitoring and anterior cingulate cortex: an update. Trends Cogn Sci. 2004; 8:539–546. [PubMed: 15556023]

Brass M, Derrfuss J, Forstmann B, von Cramon DY. The role of the inferior frontal junction area in cognitive control. Trends Cogn Sci. 2005; 9:314–316. [PubMed: 15927520]

Brodmann, K. Vergleichende Lokalisationslehre der Großhirnrinde in ihren Prinzipien dargestellt auf Grund des Zellbaues. Leipzig: Barth; 1909.

Bush G, Vogt BA, Holmes J, Dale AM, Greve D, Jenike MA, Rosen BR. Dorsal anterior cingulate cortex: a role in reward-based decision making. Proc Natl Acad Sci USA. 2002; 99:523–528. [PubMed: 11756669]

Carter CS, Braver TS, Barch DM, Botvinick MM, Noll D, Cohen JD. Anterior cingulate cortex, error detection, and the online monitoring of performance. Science. 1998; 280:747–749. [PubMed: 9563953]

Caspers J, Zilles K, Eickhoff SB, Schleicher A, Mohlberg H, Amunts K. Cytoarchitectonical analysis and probabilistic mapping of two extrastriate areas of the human posterior fusiform gyrus. Brain Struct Funct. 2013; 218:511–526. [PubMed: 22488096]

Caspers S, Eickhoff SB, Geyer S, Scheperjans F, Mohlberg H, Zilles K, Amunts K. The human inferior parietal lobule in stereotaxic space. Brain Struct Funct. 2008; 212:481–495. [PubMed: 18651173]

Caspers S, Eickhoff SB, Rick T, von Kapri A, Kuhlen T, Huang R, Shah NJ, Zilles K. Probabilistic fibre tract analysis of cytoarchitectonically defined human inferior parietal lobule areas reveals similarities to macaques. Neuroimage. 2011; 58:362–380. [PubMed: 21718787]

Cauda F, Cavanna AE, D'Agata F, Sacco K, Duca S, Geminiani GC. Functional connectivity and coactivation of the nucleus accumbens: A combined functional connectivity and structure-based meta-analysis. J Cogn Neurosci. 2011; 23:2864–2877. [PubMed: 21265603]

Chai XJ, Castanon AN, Ongur D, Whitfield-Gabrieli S. Anticorrelations in resting state networks without global signal regression. Neuroimage. 2012; 59:1420–1428. [PubMed: 21889994]

Choi HJ, Zilles K, Mohlberg H, Schleicher A, Fink GR, Armstrong E, Amunts K. Cytoarchitectonic identification and probabilistic mapping of two distinct areas within the anterior ventral bank of the human intraparietal sulcus. J Comp Neurol. 2006; 495:53–69. [PubMed: 16432904]

Cole MW, Yeung N, Freiwald WA, Botvinick M. Cingulate cortex: Diverging data from humans and monkeys. Trends Neurosci. 2009; 32:566–574. [PubMed: 19781794]

Cordes D, Haughton VM, Arfanakis K, Carew JD, Turski PA, Moritz CH, Quigley MA, Meyerand ME. Frequencies contributing to functional connectivity in the cerebral cortex in "resting-state" data. Am J Neuroradiol. 2001; 22:1326–1333. [PubMed: 11498421]

Cunnington R, Windischberger C, Deecke L, Moser E. The preparation and execution of self-initiated and externally-triggered movement: A study of event-related fMRI. Neuroimage. 2002; 15:373–385. [PubMed: 11798272]

Damoiseaux JS, Greicius MD. Greater than the sum of its parts: A review of studies combining structural connectivity and resting-state functional connectivity. Brain Struct Funct. 2009; 213:525–533. [PubMed: 19565262]

Debaere F, Wenderoth N, Sunaert S, Van Hecke P, Swinnen SP. Internal vs external generation of movements: Differential neural pathways involved in bimanual coordination performed in the presence or absence of augmented visual feedback. Neuroimage. 2003; 19:764–776. [PubMed: 12880805]

Deiber MP, Honda M, Ibanez V, Sadato N, Hallett M. Mesial motor areas in self-initiated versus externally triggered movements examined with fMRI: Effect of movement type and rate. J Neurophysiol. 1999; 81:3065–3077. [PubMed: 10368421]

Dum RP, Strick PL. The origin of corticospinal projections from the premotor areas in the frontal lobe. J Neurosci. 1991; 11:667–689. [PubMed: 1705965]

Eickhoff SB, Bzdok D, Laird AR, Kurth F, Fox PT. Activation likelihood estimation meta-analysis revisited. Neuroimage. 2012; 59:2349–2361. [PubMed: 21963913]

Eickhoff SB, Bzdok D, Laird AR, Roski C, Caspers S, Zilles K, Fox PT. Co-activation patterns distinguish cortical modules, their connectivity and functional differentiation. Neuroimage. 2011; 57:938–949. [PubMed: 21609770]

Eickhoff SB, Grefkes C. Approaches for the integrated analysis of structure, function and connectivity of the human brain. Clin EEG Neurosci. 2011; 42:107–121. [PubMed: 21675600]

Eickhoff SB, Jbabdi S, Caspers S, Laird AR, Fox PT, Zilles K, Behrens TEJ. Anatomical and functional connectivity of cytoarchitectonic areas within the human parietal operculum. J Neurosci. 2010; 30:6409–6421. [PubMed: 20445067]

Eickhoff SB, Laird AR, Grefkes C, Wang LE, Zilles K, Fox PT. Coordinate-based activation likelihood estimation meta-analysis of neuroimaging data: A random-effects approach based on empirical estimates of spatial uncertainty. Hum Brain Mapp. 2009; 30:2907–2926. [PubMed: 19172646]

Eickhoff SB, Paus T, Caspers S, Grosbras MH, Evans AC, Zilles K, Amunts K. Assignment of functional activations to probabilistic cytoarchitectonic areas revisited. Neuroimage. 2007; 36:511–521. [PubMed: 17499520]

Fox MD, Raichle ME. Spontaneous fluctuations in brain activity observed with functional magnetic resonance imaging. Nat Rev Neurosci. 2007; 8:700–711. [PubMed: 17704812]

Fox PT, Lancaster JL. Mapping context and content: the BrainMap model. Nat Rev Neurosci. 2002; 3:319–321. [PubMed: 11967563]

Friston KJ, Frith CD, Liddle PF, Frackowiak RSJ. Functional connectivity—The principal-component analysis of large (pet) data sets. J Cereb Blood Flow Metab. 1993; 13:5–14. [PubMed: 8417010]

Geyer S, Ledberg A, Schleicher A, Kinomura S, Schormann T, Burgel U, Klingberg T, Larsson J, Zilles K, Roland PE. Two different areas within the primary motor cortex of man. Nature. 1996; 382:805–807. [PubMed: 8752272]

Geyer S, Schormann T, Mohlberg H, Zilles K. Areas 3a, 3b, and 1 of human primary somatosensory cortex. Part 2. Spatial normalization to standard anatomical space. Neuroimage. 2000; 11:684–696. [PubMed: 10860796]

Greicius MD, Supekar K, Menon V, Dougherty RF. Resting-state functional connectivity reflects structural connectivity in the default mode network. Cereb Cortex. 2009; 19:72–78. [PubMed: 18403396]

Haggard P. Human volition: Towards a neuroscience of will. Nat Rev Neurosci. 2008; 9:934–946. [PubMed: 19020512]

Hoffstaedter F, Grefkes C, Zilles K, Eickhoff SB. The “what” and “when” of self-initiated movements. Cereb Cortex. 2013; 23:520–530. [PubMed: 22414772]

Holmes CJ, Hoge R, Collins L, Woods R, Toga AW, Evans AC. Enhancement of MR images using registration for signal averaging. J Comput Assist Tomogr. 1998; 22:324–333. [PubMed: 9530404]

Honey CJ, Sporns O, Cammoun L, Gigandet X, Thiran JP, Meuli R, Hagmann P. Predicting human resting-state functional connectivity from structural connectivity. Proc Natl Acad Sci USA. 2009; 106:2035–2040. [PubMed: 19188601]

Jakobs O, Langner R, Caspers S, Roski C, Cieslik EC, Zilles K, Laird AR, Fox PT, Eickhoff SB. Across-study and within-subject functional connectivity of a right temporo-parietal junction subregion involved in stimulus-context integration. Neuroimage. 2012; 60:2389–2398. [PubMed: 22387170]

Jankowski J, Scheef L, Huppe C, Boecker H. Distinct striatal regions for planning and executing novel and automated movement sequences. Neuroimage. 2009; 44:1369–1379. [PubMed: 19059350]

Johansen-Berg H, Rushworth MFS. Using diffusion imaging to study human connectional anatomy. Annu Rev Neurosci. 2009; 32:75–94. [PubMed: 19400718]

Kelly AM, Di Martino A, Uddin LQ, Shehzad Z, Gee DG, Reiss PT, Margulies DS, Castellanos FX, Milham MP. Development of anterior cingulate functional connectivity from late childhood to early adulthood. Cereb Cortex. 2009; 19:640–657. [PubMed: 18653667]

Koechlin E, Summerfield C. An information theoretical approach to prefrontal executive function. Trends Cogn Sci. 2007; 11:229–235. [PubMed: 17475536]

Kurth F, Zilles K, Fox PT, Laird AR, Eickhoff SB. A link between the systems: functional differentiation and integration within the human insula revealed by meta-analysis. Brain Struct Funct. 2010; 214:519–534. [PubMed: 20512376]

Laird AR, Eickhoff SB, Kurth F, Fox PM, Uecker AM, Turner JA, Robinson JL, Lancaster JL, Fox PT. ALE meta-analysis workflows via the brainmap database: Progress towards a probabilistic functional brain atlas. Front Neuroinform. 2009; 3:23. [PubMed: 19636392]

Laird AR, Lancaster JL, Fox PT. BrainMap—The social evolution of a human brain mapping database. Neuroinformatics. 2005; 3:65–77. [PubMed: 15897617]

Lancaster JL, Tordesillas-Gutierrez D, Martinez M, Salinas F, Evans A, Zilles K, Mazziotta JC, Fox PT. Bias between MNI and Talairach coordinates analyzed using the ICBM-152 brain template. Hum Brain Mapp. 2007; 28:1194–1205. [PubMed: 17266101]

Lau HC, Rogers RD, Ramnani N, Passingham RE. Willed action and attention to the selection of action. Neuroimage. 2004; 21:1407–1415. [PubMed: 15050566]

Margulies DS, Kelly AMC, Uddin LQ, Biswal BB, Castellanos FX, Milham MP. Mapping the functional connectivity of anterior cingulate cortex. Neuroimage. 2007; 37:579–588. [PubMed: 17604651]

Morecraft RJ, Stilwell-Morecraft KS, Cipolloni PB, Ge J, McNeal DW, Pandya DN. Cytoarchitecture and cortical connections of the anterior cingulate and adjacent somatomotor fields in the rhesus monkey. Brain Res Bull. 2012; 87:457–497. [PubMed: 22240273]

Nichols T, Brett M, Andersson J, Wager T, Poline JB. Valid conjunction inference with the minimum statistic. Neuroimage. 2005; 25:653–660. [PubMed: 15808966]

Oldfield RC. Assessment and analysis of handedness—Edinburgh inventory. Neuropsychologia. 1971; 9:97–113. [PubMed: 5146491]

Palomero-Gallagher N, Mohlberg H, Zilles K, Vogt B. Cytology and receptor architecture of human anterior cingulate cortex. J Comp Neurol. 2008; 508:906–926. [PubMed: 18404667]

Palomero-Gallagher N, Vogt BA, Schleicher A, Mayberg HS, Zilles K. Receptor architecture of human cingulate cortex: Evaluation of the four-region neurobiological model. Hum Brain Mapp. 2009; 30:2336–2355. [PubMed: 19034899]

Paus T. Primate anterior cingulate cortex: Where motor control, drive and cognition interface. Nat Rev Neurosci. 2001; 2:417–424. [PubMed: 11389475]

Reetz K, Dogan I, Rolfs A, Binkofski F, Schulz JB, Laird AR, Fox PT, Eickhoff SB. Investigating function and connectivity of morphometric findings—Exemplified on cerebellar atrophy in spinocerebellar ataxia 17 (SCA17). Neuroimage. 2012; 62:1354–1366. [PubMed: 22659444]

Robinson JL, Laird AR, Glahn DC, Lovallo WR, Fox PT. Metaanalytic connectivity modeling: delineating the functional connectivity of the human amygdala. Hum Brain Mapp. 2010; 31:173–184. [PubMed: 19603407]

Rottschy C, Langner R, Dogan I, Reetz K, Laird AR, Schulz JB, Fox PT, Eickhoff SB. Modelling neural correlates of working memory: A coordinate-based meta-analysis. Neuroimage. 2012; 60:830–846. [PubMed: 22178808]

Scheperjans F, Eickhoff SB, Homke L, Mohlberg H, Hermann K, Amunts K, Zilles K. Probabilistic maps, morphometry, and variability of cytoarchitectonic areas in the human superior parietal cortex. Cereb Cortex. 2008; 18:2141–2157. [PubMed: 18245042]

Shackman AJ, Salomons TV, Slagter HA, Fox AS, Winter JJ, Davidson RJ. The integration of negative affect, pain and cognitive control in the cingulate cortex. Nat Rev Neurosci. 2011; 12:154–167. [PubMed: 21331082]

Smith SM, Fox PT, Miller KL, Glahn DC, Fox PM, Mackay CE, Filippini N, Watkins KE, Toro R, Laird AR, Beckmann CF. Correspondence of the brain's functional architecture during activation and rest. Proc Natl Acad Sci USA. 2009; 106:13040–13045. [PubMed: 19620724]

Smith SM, Miller KL, Salimi-Khorshidi G, Webster M, Beckmann CF, Nichols TE, Ramsey JD, Woolrich MW. Network modelling methods for FMRI. Neuroimage. 2011; 54:875–891. [PubMed: 20817103]

Turkeltaub PE, Eickhoff SB, Laird AR, Fox M, Wiener M, Fox P. Minimizing within-experiment and within-group effects in activation likelihood estimation meta-analyses. Hum Brain Mapp. 2012; 33:1–13. [PubMed: 21305667]

Van Dijk KR, Hedden T, Venkataraman A, Evans KC, Lazar SW, Buckner RL. Intrinsic functional connectivity as a tool for human connectomics: theory, properties, and optimization. J Neurophysiol. 2010; 103:297–321. [PubMed: 19889849]

van Eimeren T, Wolbers T, Munchau A, Buchel C, Weiller C, Siebner HR. Implementation of visuospatial cues in response selection. Neuroimage. 2006; 29:286–294. [PubMed: 16087350]

Vogt BA. Pain and emotion interactions in subregions of the cingulate gyrus. Nat Rev Neurosci. 2005; 6:533–544. [PubMed: 15995724]

Vogt, BA. Architecture, neurocytology and comparative organization of monkey and human cingulate cortices. In: Vogt, BA., editor. Cingulate Neurobiology and Disease. Oxford; New York: Oxford University Press; 2009a. p. 65-94.

Vogt, BA. Regions and subregions of the cingulate gyrus. In: Vogt, BA., editor. Cingulate Neurobiology and Disease. Oxford; New York: Oxford University Press; 2009b. p. 4-30.

Vogt BA, Berger GR, Derbyshire SW. Structural and functional dichotomy of human midcingulate cortex. Eur J Neurosci. 2003; 18:3134–3144. [PubMed: 14656310]

Vogt, BA., Hof, PR., Vogt, LJ. Cingulate gyrus. In: Paxinos, G., Mai, JK., editors. The Human Nervous System. Amsterdam: Elsevier; 2004. p. 915-949.

Vogt BA, Pandya DN. Cingulate cortex of the rhesus-monkey. 2. Cortical afferents. J Comp Neurol. 1987; 262:271–289. [PubMed: 3624555]

Vogt BA, Vogt L. Cytology of human dorsal midcingulate and supplementary motor cortices. J Chem Neuroanat. 2003; 26:301–309. [PubMed: 14729132]

Weissenbacher A, Kasess C, Gerstl F, Lanzenberger R, Moser E, Windischberger C. Correlations and anticorrelations in resting-state functional connectivity MRI: A quantitative comparison of preprocessing strategies. Neuroimage. 2009; 47:1408–1416. [PubMed: 19442749]

Yarkoni T, Poldrack RA, Nichols TE, Van Essen DC, Wager TD. Large-scale automated synthesis of human functional neuroimaging data. Nat Methods. 2011; 8:665–670. [PubMed: 21706013]

Yu C, Zhou Y, Liu Y, Jiang T, Dong H, Zhang Y, Walter M. Functional segregation of the human cingulate cortex is confirmed by functional connectivity based neuroanatomical parcellation. Neuroimage. 2011; 54:2571–2581. [PubMed: 21073967]

Zilles K, Amunts K. Centenary of Brodmann's map–Conception and fate. Nat Rev Neurosci. 2010; 11:139–145. [PubMed: 20046193]

zu Eulenburg P, Caspers S, Roski C, Eickhoff SB. Meta-analytical definition and functional connectivity of the human vestibular cortex. Neuroimage. 2012; 60:162–169. [PubMed: 22209784]

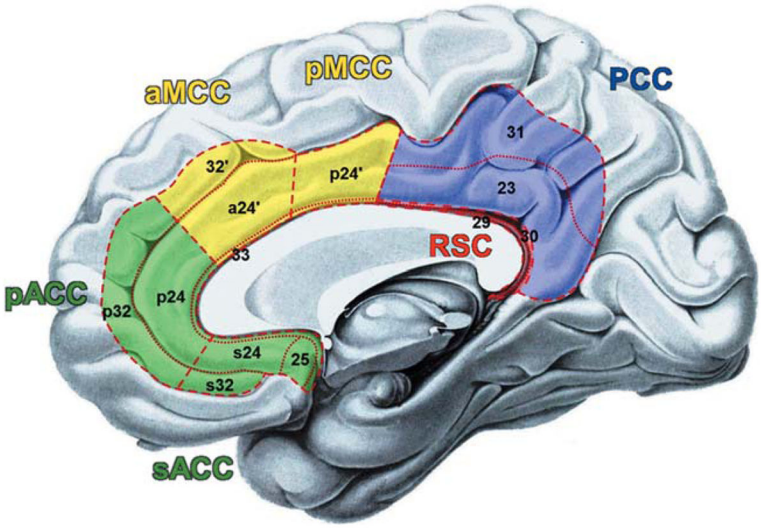

Figure 1.

Schematic drawing of the four region model of the cingulate cortex according to Vogt et al. [2004]: (I) the anterior cingulate cortex (ACC) in green comprises the perigenual (pACC: areas p32, p24) and the subgenual (sACC: areas s32, s24, 25) subregion; (II) the midcingulate cortex (MCC) in yellow subdivided into an anterior (aMCC: areas a24′, 32′) and a posterior (pMCC; area p24′) part; (III) the posterior cingulate cortex (PCC: areas 23, 32) in blue; (IV) the retrosplenial cortex (RSC: 29, 30) in red. Dashed lines indicate regional borders and dotted lines highlight areal borders.

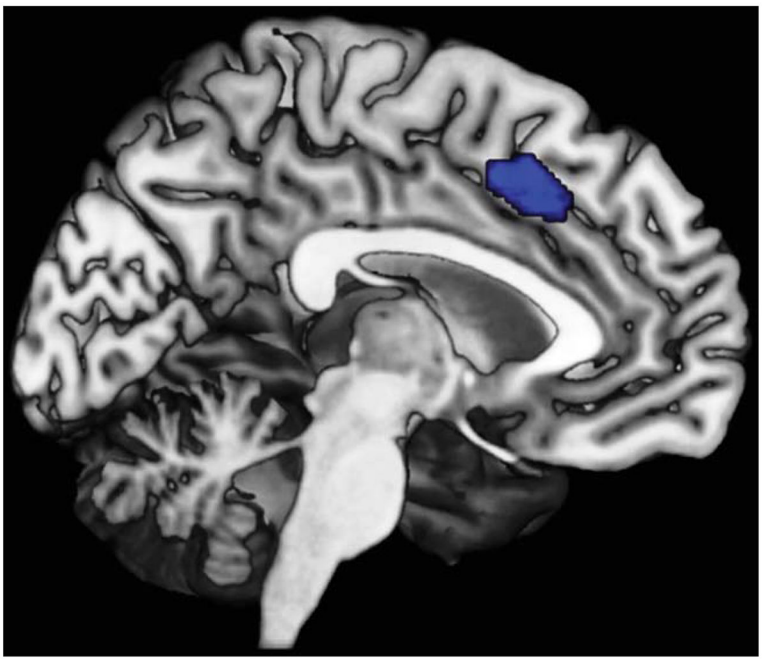

Figure 2.

Anterior midcingulate cortex region involved in both the intentional selection and timing of movement initiation (median MNI coordinate: $x = -3$; $y = 18$; $z = 42$; volume = 1,873 mm^3 [Hoffstaedter et al., 2013]) used as seed volume of interest (VOI) in MACM and resting-state analysis.

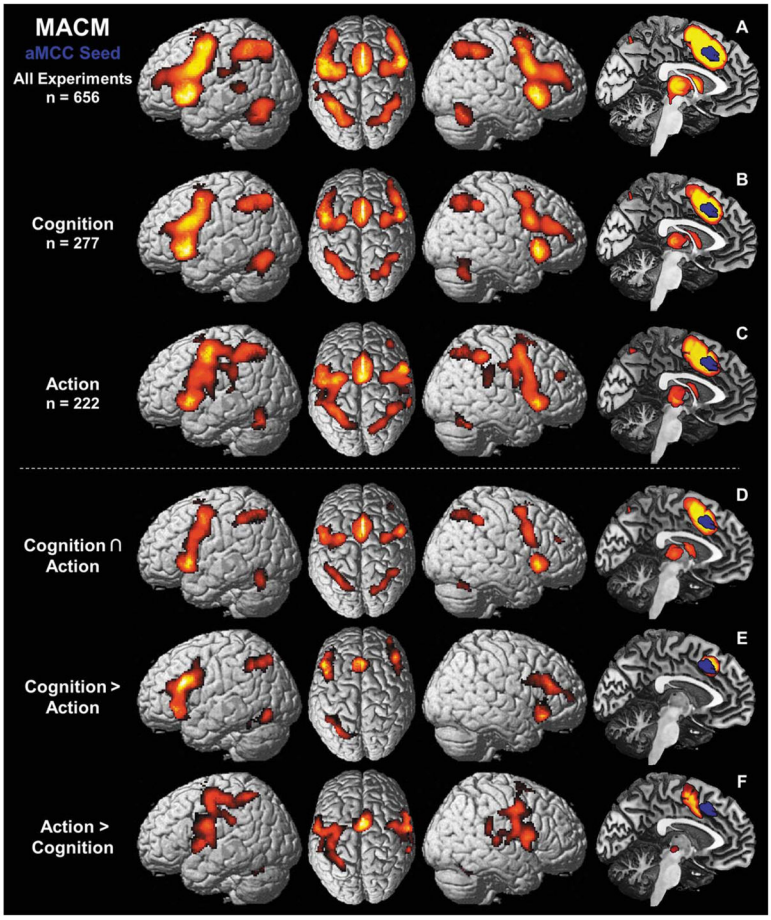

Figure 3.

Results of the meta-analytic connectivity modeling (MACM) showing regions of convergent co-activation with the aMCC seed VOI (in blue) over various different task conditions. (**A**) Task-based functional connectivity (FC) of aMCC independent of domain. (**B**) FC of aMCC with regard to the behavioral domain “cognition” as defined by the BrainMap database [Laird et al., 2009]. (**C**) FC of aMCC over experiments examining “action” as behavioral domain. **D**) Conjunction over task-base FC of aMCC with regard to “cognition” (B) and to “action” (C), respectively. (**E**) Higher task-based FC of aMCC over experiments related to “cognition” than “action.” (**F**) Higher task-based FC of aMCC over experiments examining “action” than examining “cognition.”

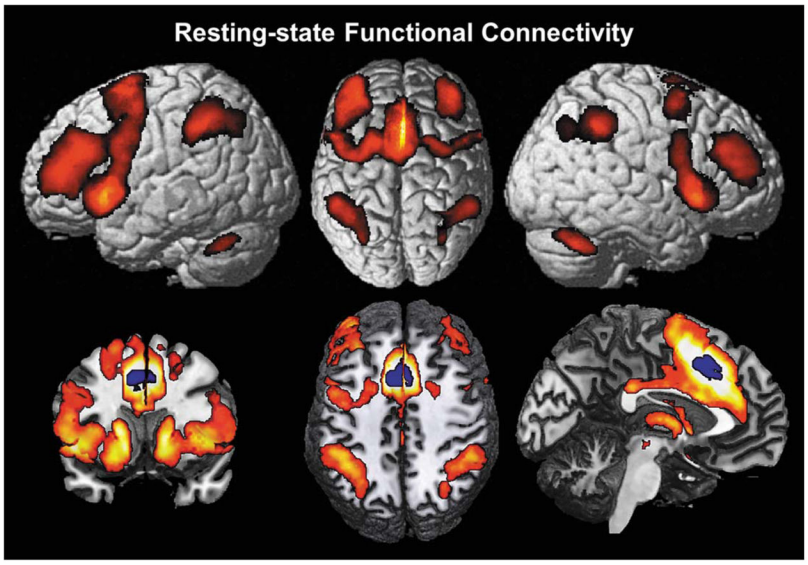

Figure 4.
Results of the seed based resting-state analysis showing regions of functional connectivity, i.e., significantly correlated fluctuations of the BOLD-activity with the aMCC VOI over 100 subjects.

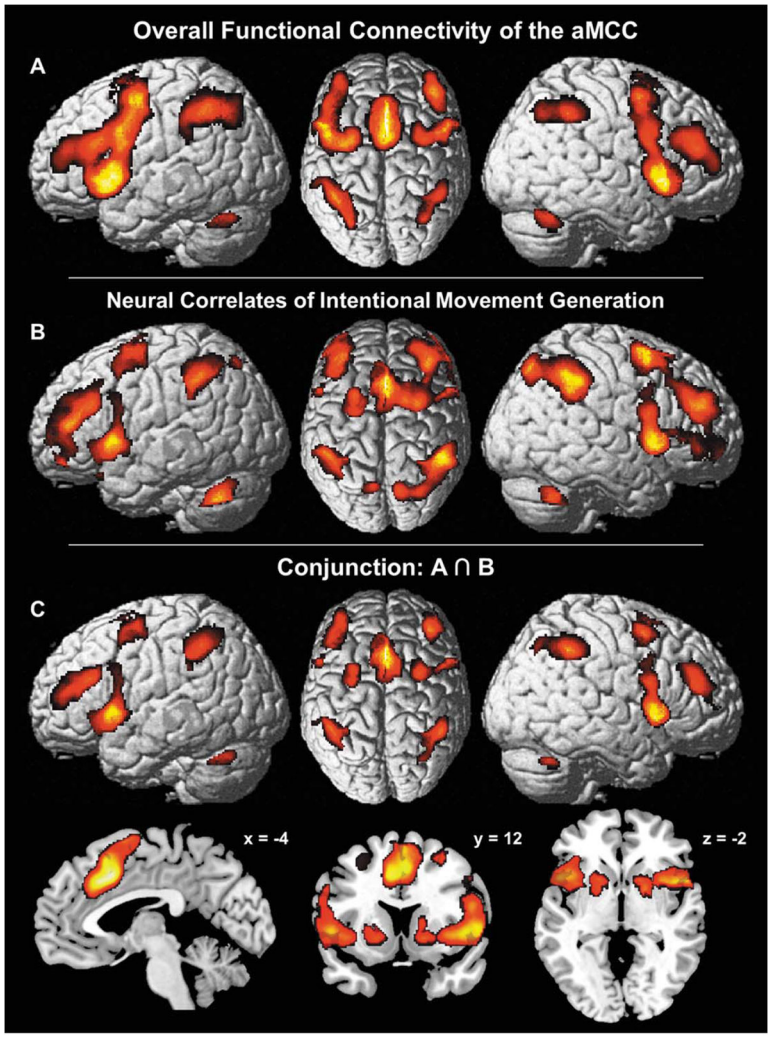

Figure 5.

Comparison of the aMCC's overall functional connectivity (FC) with neural correlates of intentional movement generation. (**A**) Overlap between the results of MACM and the seed based resting-state analysis representing FC of the aMCC independent of context. (**B**) Neural correlates of intentional movement generation [Hoffstaedter et al., 2012] as prototypical interaction) between cognitive and motor functions. (**C**) Conjunction over the aMCC's FC independent of "state" (A) with neural correlates of intentional (cognitive) motor control (B).